

# Two-Section Impedance Transformer Design and Modeling for Power Amplifier Applications

Sobhan Roshani\* and Saeed Roshani

Department of Electrical Engineering, Kermanshah Branch, Islamic Azad University, Kermanshah, Iran

**Abstract** — In this paper, two-section impedance transformer network (TSITN) is modeled and used for power amplifiers applications. The artificial neural network (ANN) is used to propose an appropriate model for TSITN. The proposed model could predict the desired input and output impedances at desired frequencies using TSITN dimensions, which could be suitable for input and output matching network of a power amplifier. Using two-section impedance transformer network instead of conventional impedance transformer network (ITN) could miniaturize the input and output matching network size.

**Index Terms** — Matching network, neural network, power amplifier, two-section impedance transformer network.

## I. INTRODUCTION

Conventional transformers, like quarter-wave impedance transformer, suffer from several disadvantages, such as narrow bandwidth and large size [1-2]. The two-section transformer is firstly proposed in [3], which could operate at main frequency and its second harmonic. In [1], a TSITN is analyzed and the closed form equations are obtained for resistive real impedance matching. In [4], the TSITN working at two arbitrary frequencies is studied and analyzed. The main problem of these typical two-section transformers is that they are only analyzed and designed to transfer impedance to only resistive real impedance. However, according to the load pull and source pull analyses in power amplifier applications, complex impedance with real and imaginary parts is needed.

A TSITN, which could be used in dual band systems, is reported in [5]. The presented TSITN could match two complex impedances at two different frequencies. Another ITN is presented in [6]. The presented ITN in this work could match two frequency variant complex impedances at two different frequencies. This ITN could be used for power amplifier circuits with frequency variant load impedances.

A Quad-Band Four-Section ITN is designed and analyzed in [7], however the equations are complicated

and PSO optimization algorithm is used to find the required design parameters. The PSO algorithm is also used in [8] to find the design parameters of the ITN.

So far, impedance transformer networks have been used in several microwave devices, such as: power amplifiers [9-11], LNAs [12], phase shifters [13] and other microwave devices.

In power amplifiers applications, transformer networks are commonly used for Doherty power amplifiers; however, they could be used for any types of amplifiers, such as class A and other classes of amplifiers. In most of the cited works, the TSITN is only analyzed for matching at resistive real impedance, which is not suitable for power amplifier applications. Also, a few approaches provide analyses of two-section ITN and other types of ITN for complex impedances matching with time consuming numerical calculations [5], [14-16]. To the best knowledge of the authors, there is not any approach to derive the closed form equations for analysis of TSITN for complex impedances matching applications.

According to the mentioned problems for two-section transformers, a model which could predict the desired input and output impedances at desired frequencies using TSITN dimensions is still matter of challenge and discussion. In this paper, two ANN models are proposed for TSITN for power amplifier applications. The proposed models could predict the specifications of TSITN, which ease the design process of the amplifier input and output matching circuits.

## II. TWO-SECTION ITN

A typical TSITN is depicted in Fig. 1. The TSITN includes two transmission lines with different dimensions. The transformer network could match input impedance of  $Z_{in}$  to output impedance of  $Z_{out}$ . Therefore, this network could be used in the input or the output of the circuits like power amplifiers. This network is suitable to match the obtained impedance from source pull or load pull analyses to the desired circuit. The relation between input and output impedances in Fig. 1 can be defined as:

$$Z_{out2} = Z_2 \frac{Z_{out} + jZ_2 \tan(\theta_2)}{Z_2 + jZ_{out} \tan(\theta_2)}, \quad (1)$$

$$Z_{in} = Z_1 \frac{Z_{out2} + jZ_1 \tan(\theta_1)}{Z_1 + jZ_{out2} \tan(\theta_1)}, \quad (2)$$

where,  $Z_{in}$  and  $Z_{out}$  are complex impedances. The other parameters in Equations (1) and (2) are defined in Fig. 1. As seen in these equations, there are four variables ( $Z_1$ ,  $\theta_1$ ,  $Z_2$  and  $\theta_2$ ) within two equations, so, there is no unique answer to TSITN dimensions. Subsequently, the ANN modelling is presented in this paper, to predict the TSITN dimensions. A typical power amplifier matching network is shown in Fig. 2 (a). As can be seen in this figure, the output matching network should match  $Z_{load}$  to  $Z_0$  at the drain of the active device. Also, the input matching network should match  $Z_{source}$  to  $Z_0$  at the gate of the active device. According to Fig. 2 (b), two-section ITN could be applied at the input and output of the circuit to match the desired impedance.

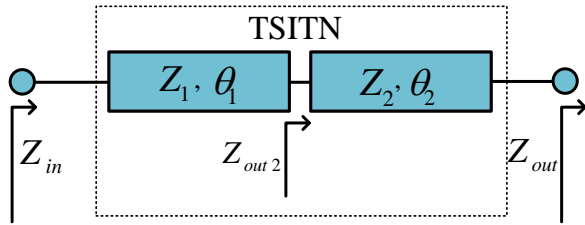


Fig. 1. A typical TSITN.

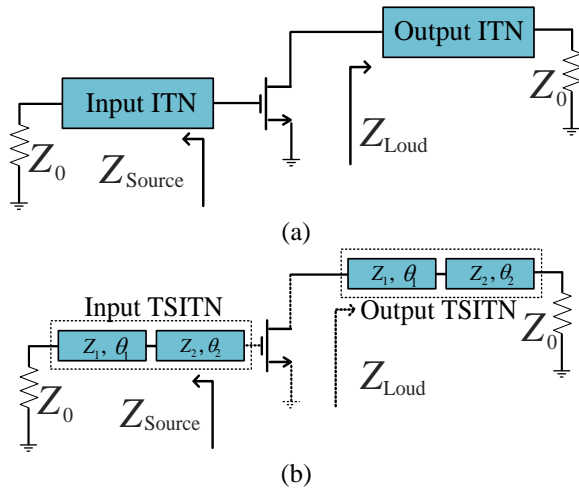


Fig. 2. (a) A typical power amplifier matching network. (b) Applied TSITN for matching network of the power amplifier.

### III. PRESENTED ANN MODEL FOR TSITN

As shown in Fig. 2, the TSITN could be used as input or output matching network. For the case in which TSITN is considered as the output matching circuit of the amplifier, the value of  $Z_{out}$  in Fig. 1 is considered as  $Z_0$ , while  $Z_{in}$  in Fig. 1 is considered as complex impedance. Design of TSITN for input matching of the power

amplifier is similar to design of TSITN for output matching, so, only design and modeling of TSITN for output matching is considered, in this paper. For prediction of the desired  $Z_{in}$ , an ANN model of TSITN is proposed, as shown in Fig. 3. According to this model, the desired complex impedance in any frequency could be predicted, using dimensions of the TSITN. The frequency is arbitrary parameter in the presented model; therefore, this model could be used in any power amplifier circuits. A TSITN is simulated and designed in computer aided design software, advanced design system (ADS) 2008, to acquire the database for the proposed ANN model. The TSITN is simulated in ADS schematic design section using S-parameters analysis. The S-parameter analysis in ADS could calculate the scattering parameters (S-parameters) of a circuit and convert scattering parameters to Z-parameters. After simulating several TSITNs with different dimensions and obtaining the impedances in different frequencies, 150 data of input and output parameters are extracted to form the database. The TSITN is modeled with multi-layer perceptron (MLP) and radial basis function (RBF) networks in this paper, which will be described in subsections A and B, respectively. The proposed ANN networks are trained and tested using MATLAB R2012b software. The MATLAB built-in functions of "newff" and "newrb" are utilized in the proposed MATLAB codes for MLP and RBF networks, respectively.

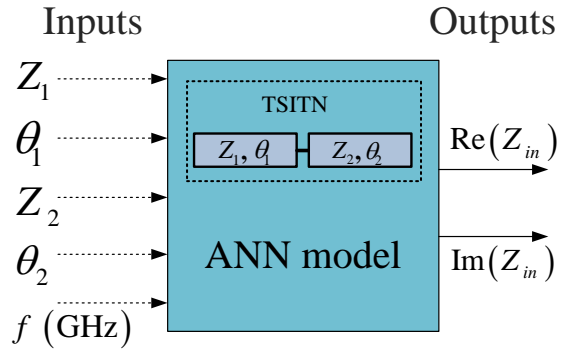


Fig. 3. The proposed ANN model for TSITN.

#### A. MLP network

MLP neural network is a feedforward network, which uses backpropagation algorithm for finding the weights between neurons. The MLP network has three main layers (input, hidden and the output layers). The hidden layer may include one layer or several layers. The number of hidden layers is chosen, according to the problem and data set. In most of applications, high precision could be achieved with only one layer or two layers [17]. The neuron numbers in the ANN layers can be selected proportional to the data and the number of output/input parameters. Higher number of neurons or hidden layers may increase the accuracy of the network,

but it could raise the complexity and simulation time of the network. MLP networks are presented, according to conditions of the defined network shown in Fig. 3. Several MLP structures have been tested and the best network is chosen to model the presented circuit. The total number of data set is 150, which is constant during the simulation in all of the ANNs, in this paper. The data are normalized and about 80% of data are considered for testing and the rest are considered for training process. Several MLP structures with different number of neurons and hidden layers are tested, to find the best network. Error results of different MLP structures are shown in Table 1. Each network is applied 100 times with number of epoch 3000 and the best error results are listed in the table. Mean absolute and root mean squared errors (MAE and RMSE) of different presented networks are reported in this paper to compare the precision of the networks. The errors for each considered output is reported in Table 1. Effects of different number of neurons on the MLP networks MAE are shown in Fig. 4. According to Fig. 4, approximately, the errors decrease, as the number of neurons increases. However, high number of layers and neurons increase the simulation time and complexity of the network and may result in over-fitting of the network. Therefore, the network with 7 neurons in each layer is assumed as the best structure with the best error results. The best configuration for the presented MLP is shown in Fig. 5.

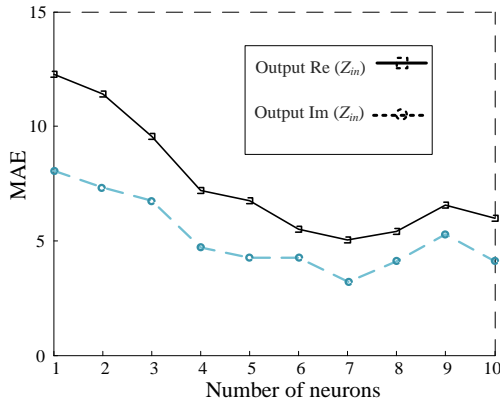


Fig. 4. The MAE of MLP networks versus different number of neurons.

In this paper, MAE and RMSE errors are calculated for all of the presented neural networks, using the following equations:

$$MAE = \frac{\sum_{i=1}^N |Y_{Rei} - Y_{Pri}|}{N}, \tag{3}$$

$$RMSE = \sqrt{\frac{\sum_{i=1}^N (Y_{Rei} - Y_{Pri})^2}{N}}. \tag{4}$$

In Equations (3) and (4),  $N$  is total number of data, while  $Y_{Rei}$  and  $Y_{Pri}$  are respectively, real and predicted outputs of the network. Real and predicted values of  $Re(Z_{in})$  and  $Im(Z_{in})$  for the best obtained MLP networks are shown in Figs. 6 and 7, respectively. According to these figures, the presented MLP model has modeled the TSITN, accurately.

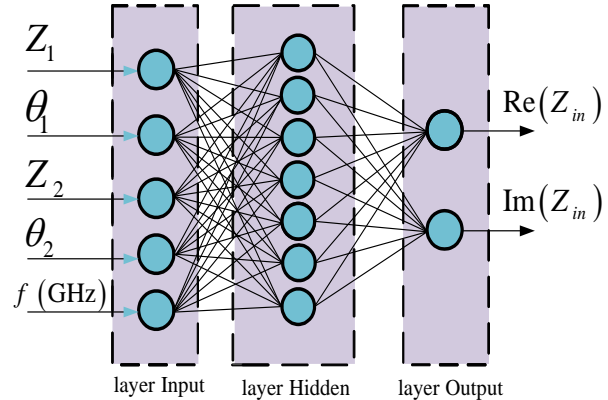


Fig. 5. Structure of the best presented MLP neural network.

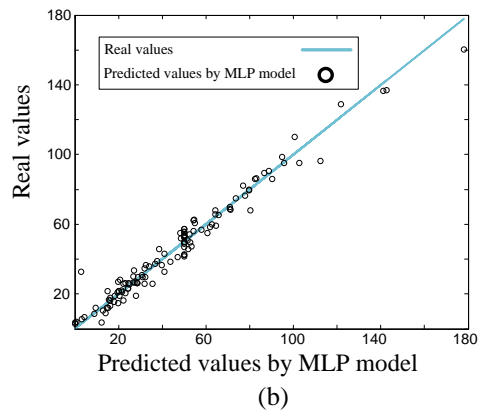
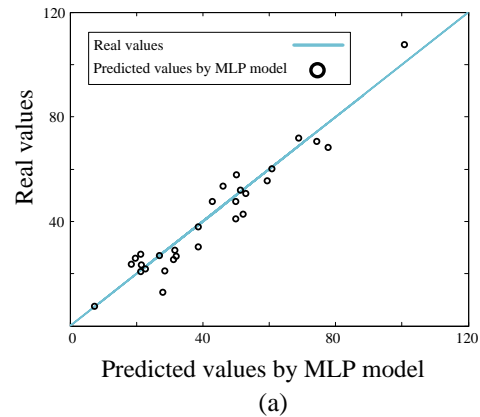


Fig. 6. Real and predicted values comparison, using the best obtained MLP structure for real part of  $Z_{in}$ : (a) test and (b) train data.

Table 1: Obtained results for different structures of MLP networks

Number of Neurons	MAE Test-Re (Zin)	RMSE Test-Re (Zin)	MAE Test-Im (Zin)	RMSE Test-Im (Zin)
1	12.27	18.48	8.05	13.74
2	11.41	18.18	7.34	9.39
3	9.56	18.43	6.75	8.18
4	7.20	12.71	4.70	7.08
5	6.75	8.59	4.26	5.42
6	5.50	8.07	4.25	5.91
7	5.15	6.38	3.61	4.73
8	5.40	7.06	4.10	8.20
9	6.55	8.55	5.27	7.77
10	5.99	9.89	4.10	6.13

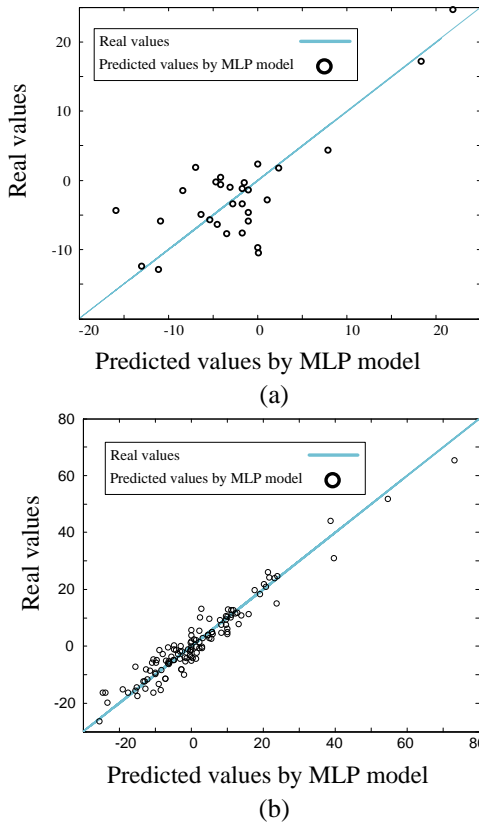


Fig. 7. Real and predicted values comparison, using the best obtained MLP structure for imaginary part of  $Z_{in}$ : (a) test and (b) train data.

**B. RBF network**

RBF ANN is a feedforward ANN and its structure is similar to MLP network. However, the RBF network has one hidden layer and the activation functions are radial basis functions [18]. Conventional structure of a RBF ANN is depicted in Fig. 8. The outputs of neurons in hidden layer will be summed, by the output layer neurons. This procedure is defined in Equations (5) and (6):

$$q_i = \exp\left(-\frac{\|X_i - C_i\|^2}{\sigma_i^2}\right), \tag{5}$$

$$y = \sum_{i=1}^n w_i q_i. \tag{6}$$

In Equations (5) and (6), the parameter  $X$  shows input vector of the hidden layer,  $y$  shows output of the network,  $C$  is center of the basis function and  $\sigma$  is the Gaussian function spread. Parameters of presented RBF model is listed in Table 2. The obtained results of the presented RBF model is listed in Table 3.

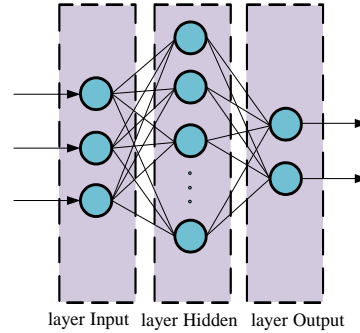


Fig. 8. Typical RBF structure.

Table 2: Parameters of presented RBF model

Hidden layer function	Radial basis
Output layer function	Linear
Input neuron numbers	5
Output neuron numbers	2
Maximum number of neurons	100
Train data numbers	120
Test data numbers	30

**IV. RESULTS OF THE PROPOSED MODELS**

The obtained RMSE and MAE results of the presented models using MLP and RBF ANNs are listed in Table 3. The errors are reported for both real and imaginary parts of the predicted  $Z_{in}$ . According to the results, two proposed MLP and RBF networks have modeled the TSITN in different frequency ranges, precisely.

Table 3: Obtained results for presented MLP and RBF networks

Errors	ANN	
	MLP	RBF
MAE-train for Re ( $Z_{in}$ )	3.97	0.11
MAE-train for Im ( $Z_{in}$ )	2.90	0.11
MAE-test for Re ( $Z_{in}$ )	5.15	7.85
MAE-test for Im ( $Z_{in}$ )	3.61	4.86
RMSE-train for Re ( $Z_{in}$ )	5.59	0.22
RMSE-train Im ( $Z_{in}$ )	3.76	0.20
RMSE-test for Re ( $Z_{in}$ )	6.38	14.31
RMSE-test for Im ( $Z_{in}$ )	4.73	8.36

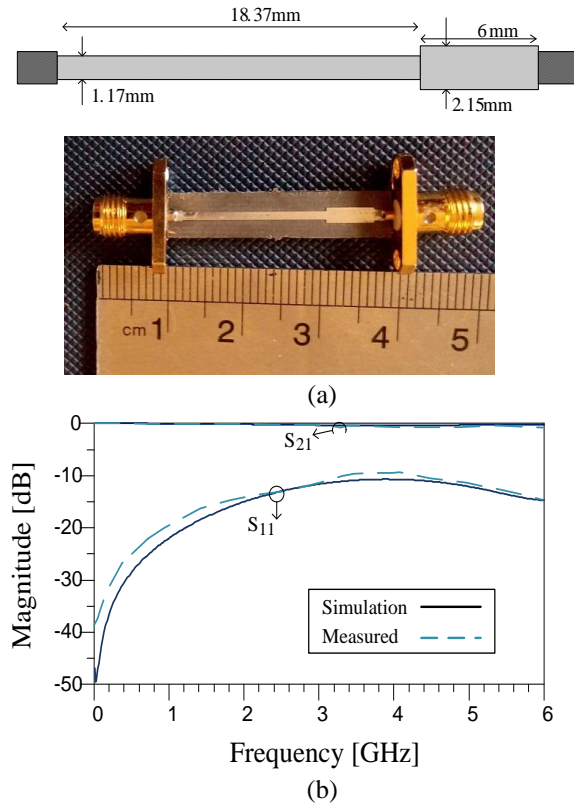


Fig. 9. (a) Layout, photograph, and (b) frequency response of the fabricated impedance transformer.

#### A. Data validation

For validation of the impedance transformer network proposed model, the data of a sample TSITN is applied to the proposed model. The layout and photograph of the fabricated TSITN are depicted in Fig. 9 (a). The obtained  $S_{11}$  and  $S_{21}$  of the fabricated TSITN are illustrated in Fig. 9 (b). The specifications of the applied substrate is  $\epsilon_r = 2.2$  and thickness = 0.508 mm. This TSITN transfers  $50 \Omega$  output matching port to  $(52.23 + 7.67j) \Omega$  in the output of the desired power amplifier at 1 GHz. After applying this data to the proposed MLP model, the predicted value was obtained  $(42.65 + 9.59j) \Omega$ , which shows acceptable accuracy for validation data.

#### V. CONCLUSION

In this paper, MLP and RBF networks are presented to model two-section impedance transformer network for power amplifier and impedance matching applications. The presented models could describe the impedance transformer network behavior versus the different frequencies. Compared to the other impedance transformer design approaches in which the complicated and time consuming equations should be solved for finding the design parameters, the presented model can easily predict the design parameters of impedance transformer using artificial neural networks. Several

structures have been tested to find the best network, which can model the presented impedance transformer, accurately. Finally, data of a fabricated transformer is applied to the proposed model. The results show that the presented model is accurate and could be considered as reliable model for high frequency amplifiers with desired transforming matching values.

#### ACKNOWLEDGMENT

The authors would like to thank the Kermanshah Branch, Islamic Azad University for the financial support of this research project.

#### REFERENCES

- [1] C. Monzon, "Analytical derivation of a two-section impedance transformer for a frequency and its first harmonic," *IEEE Microw. Wireless Comp. Lett.*, vol. 12, pp. 381-382, 2002.
- [2] T. K. Ishii, *Microwave Engineering*. Oxford University Press on Demand, 1989.
- [3] Y. L. Chow and K. L. Wan, "A transformer of one-third wavelength in two sections for a frequency and its first harmonic," *IEEE Microw. Wireless Comp. Lett.*, vol. 12, no. 1, pp. 22-23, 2002.
- [4] C. Monzon, "A small dual-frequency transformer in two sections," *IEEE Trans. Microwave Theory Tech.*, vol. 51, pp. 1157-1161, 2003.
- [5] Y. Wu, Y. Liu, and S. Li, "A dual-frequency transformer for complex impedances with two unequal sections," *IEEE Microw. Wireless Comp. Lett.*, vol. 19, pp. 77-79, 2009.
- [6] X. Liu, Y. A. Liu, S. Li, F. Wu, and Y. A. Wu, "Three-section dual-band transformer for frequency-dependent complex load impedance," *IEEE Microw. Wireless Comp. Lett.*, vol. 19, pp. 611-613, 2009.
- [7] H. Jwaied, F. Muwanes, and N. Dib, "Analysis and design of quad-band four-section transmission line impedance transformer," *Applied Computational Electromagnetics Society (ACES) Journal*, vol. 22, no. 3, pp. 381-387, 2007.
- [8] M. Khodier, "Design and optimization of single, dual, and triple band transmission line matching transformers for frequency-dependent loads," *Applied Computational Electromagnetics Society (ACES) Journal*, vol. 24, no. 5, pp. 446-452, 2009.
- [9] M. Hayati and S. Roshani, "A broadband Doherty power amplifier with harmonic suppression," *AEU-Int. J. Electron. C.*, vol. 68, pp. 406-412, 2014.
- [10] P. Saad, P. Colantonio, L. Piazzon, F. Giannini, K. Andersson, and C. Fager, "Design of a concurrent dual-band 1.8-2.4-GHz GaN-HEMT Doherty power amplifier," *IEEE Trans. Microwave Theory Tech.*, vol. 60, pp. 1840-1849, 2012.
- [11] M. Hayati and S. Roshani, "A novel miniaturized

power amplifier with nth harmonic suppression,” *AEU-Int. J. Electron. C.*, vol. 68, pp. 1016-1021, 2014.

- [12] P. Mousavi, M. Fakharzadeh, S. H. Jamali, K. Narimani, M. Hossu, H. Bolandhemmat, G. Rafi, and S. Safavi-Naeini, “A low-cost ultra low profile phased array system for mobile satellite reception using zero-knowledge beamforming algorithm,” *IEEE Trans. Antennas Propag.*, vol. 56, no. 12, pp. 3667-3679, 2008.
- [13] P. Mousavi, I. Ehtezazi, S. Safavi-Naeini, and M. Kahrizi, “A new low cost phase shifter for land mobile satellite transceiver,” *IEEE Antennas and Propagation Society International Symposium*, vol. 2, pp. 229-232, July 2005.
- [14] Q. He, Y. Liu, M. Su, and Y. Wu, “A compact dual-frequency transformer for frequency-dependent complex impedance load,” in *IEEE Asia-Pacific Microwave Conference Proceedings (APMC)*, pp. 1241-1243, 2012.
- [15] Y. Wu, Y. Liu, S. Li, C. Yu, and X. Liu, “A generalized dual-frequency transformer for two arbitrary complex frequency-dependent impedances,” *IEEE Microw. Wireless Comp. Lett.*, vol. 19, no. 12, pp. 792-794, 2009.
- [16] R. K. Barik, P. K. Bishoyi, and S. S. Karthikeyan, “Design of a novel dual-band impedance transformer,” in *IEEE Conference on Electronics, Computing and Communication Technologies (CONECCT)*, pp. 1-4, July 2015.
- [17] M. Hayati, F. Shama, S. Roshani, and A. Abdipour, “Linearization design method in class-F power amplifier using artificial neural network,” *J. Comput. Electron.*, vol. 13, pp. 943-949, 2014.
- [18] W. Yao, J. Fang, P. Zhao, S. Liu, J. Wen, and S. Wang, “TCSC nonlinear adaptive damping controller design based on RBF neural network to enhance power system stability,” *J. Electr. Eng. Technol.*, vol. 8, pp. 252-261, 2013.



**Sobhan Roshani** received the B.Sc. degree in Electrical Engineering from Razi University, Kermanshah, Iran in 2010, M.Sc. degree in Electrical Engineering from Iran University of Science & Technology - IUST, Tehran, Iran in 2012 and Ph.D. in Electrical Engineering from Razi University in 2016. His research interest includes switching power amplifiers, microwave circuits, optimization and neural networks.



**Saeed Roshani** received the B.Sc. degree in Electrical Engineering from Razi University, Kermanshah, Iran in 2008, M.Sc. degree in Electrical Engineering from Shahed University, Tehran, Iran in 2011 and Ph.D. in Electrical Engineering from Razi University in 2015. He has published more than 40 papers in ISI Journals and Conferences and two books. His research interest includes the microwave and millimeter wave devices and circuits.